consistent with a high condensation degree of the samples.

(d) Peaks corresponding to the alkene C atoms in 3-MPS are retained in the polymer samples (Table IV), which suggests that vinylic polymerization did not take place under the conditions of the present study. In fact, no NMR observation allows us to conclude on this reaction.

Conclusions

The aim of this work was to prepare specific materials usable in membrane technologies. As illustrated in this paper, a large variety of molecular precursors can be combined in order to prepare tailored organic–inorganic polymers such as heteropolysiloxanes.

An NMR investigation showed that condensation of heteropolysiloxanes from alkoxysilanes can be successfully completed providing that reaction conditions are adaptable to the different precursors.

From a chemical point of view, some important conclusions can be drawn for the preparation of these heteropolysiloxanes: replacement of PAN by PYDAN stops the condensation at an average condensation degree of about $n = 2.2$; full condensation $n = 3$) is attained after a 7 h reaction time for the first step; high temperature (80 °C) and EtOH as solvent instead of $CHCl_3$ favor full condensation (In the early stages, however, EtOH gives rise to side reactions. A change of solvent would therefore be the method of choice.); the thermal treatment at 120 °C partially degrades the polymer backbone and should therefore be replaced by an alternative curing procedure.

Acknowledgment. Liquid NMR spectra were recorded on the spectrometer of the "Service Commun de RMN" University of Montpellier. Financial support in the framework of an "Action Intégrée" between France and Spain is gratefully acknowledged.

Registry No. (3-APS)(PAN) (copolymer), 131618-03-6; (3-APS)-(PYDAN) (copolymer), 131618-04-7; (3-APS)(PAN)(3-MPS)(TIPOT) (copolymer), 131618-05-8; (PAN)(3-APS)(3-MPS)(MTMS)(TIPOT) (copolymer), 131618-06-9; (PAN)(3-APS)(3-MPS) (copolymer), 131618-07-0; (PAN)(3-APS)(3-MPS)(MTMS) (copolymer), 131618-08-1.

Orientation and Dynamics of β-Dodecyl Glucopyranoside in Phospholipid Bilayers by Oriented Sample NMR and Order Matrix Analysis

Charles R. Sanders, II, and James H. Prestegard*

Contribution from the Department of Chemistry, Yale University, New Haven, Connecticut 06511.
Received July 9, 1990

Abstract: The structure of the glycolipid analogue β-D-dodecyl glucopyranoside (BDOG) in a phospholipid bilayer environment is presented. Isotopically labeled BDOG was synthesized, solubilized in a magnetically orientable membrane system composed of 1,2-dimyristoyl-*sn*-3-glycerophosphocholine (DMPC) and 3-[(cholamidopropyl)dimethylammonio]-2-hydroxy-1-propanesulfonate (CHAPSO), and examined by an array of 1-D and 2-D NMR methods. This allowed measurement of two quadrupolar coupling constants for glucose ring deuterons, five ^{13}C–^{1}H dipolar splittings, and six ^{13}C–^{13}C dipolar splittings. Furthermore, manipulation of the sample to monotonically scale down the anisotropic part of the nuclear spin interactions permitted the absolute signs of most of the coupling constants to be determined. This set of data allowed analysis of the full order matrix for the system and subsequent determination of the average orientation of the glucose ring with respect to the bilayer normal. The results indicate that the glucose ring is extended from the plane of the bilayer with the vector between carbons 2 and 6 approximately parallel to the plane. Motions of the ring perpendicular to the normal are restricted in an anisotropic manner, apparently to avoid placing either the 2- or 6-substituents into apolar regions of the membrane. While the average orientation is similar to that obtained by assuming axial symmetry and a single order parameter, the complete analysis offers important insight into the degree and nature of motions executed at the surface of membranes.

The dynamics, three-dimensional structure, and orientation of the carbohydrate portions of membrane-associated glycoforms (glycolipids and glycoproteins) are matters of importance given the role these molecules play in cell surface recognition events such as the binding of toxins, lectins, antibodies, and other cells.[1] Characterization of their properties is also of importance in understanding how oligosaccharides are biosynthesized at the membrane surface,[2-4] how the toxicity of bacterial lipopolysaccharides arises, and what role the glycosylphosphatidylinositol anchor plays in the association of many peripheral proteins with membrane surfaces.[5]

Structural studies of oligosaccharides that require chemical or enzymic cleavage to solubilize or facilitate crystallization of the oligosaccharide have contributed much to our current knowledge. X-ray crystal structures of complex saccharides are relatively rare, but data obtained for simple mono- and disaccharides[6] provide important building blocks for further computational and experimental studies. High-resolution NMR has provided structures for somewhat larger molecules and some insight into allowed solution conformations.[7-11] The fundamental validity of the

(1) (a) Bock, G., Harnet, S., Eds. *Carbohydrate Recognition and Cellular Function*; CIBA Foundation Symposium 145; Wiley: New York, 1989. (b) Curatolo, W. *Biochim. Biophys. Acta* **1987**, *906*, 137–160. (c) Rademacher, T. W.; Parekh, R. B.; Dwek, R. A. *Annu. Rev. Biochem.* **1988**, *57*, 785–838.
(2) Lezica, R. P.; Daleo, G. R.; Dey, P. M. *Adv. Carbohydr. Chem. Biochem.* **1986**, *44*, 341–385.
(3) Presper, K. A.; Heath, H. C. *Enzymes (3rd Ed.)* **1983**, *16*, 449–488.
(4) Kishimoto, Y. *Enzymes (3rd Ed.)* **1983**, *16*, 357–407.
(5) (a) Low, M. G. *Fed. Am. Soc. Exp. Biol. J.* **1989**, *3*, 1600–1608. (b) Thomas, J. R.; Dwek, R. A.; Rademacher, T. W. *Biochemistry* **1990**, *29*, 5413–5422.
(6) Jeffrey, G. A. *Acta Crystallogr.* **1990**, *B46*, 89–103.
(7) Homans, S. W.; Dwek, R. A.; Rademacher, T. W. *Biochemistry* **1987**, *26*, 6571–6578.
(8) Homans, S. W. *Prog. NMR Spectrosc.* **1990**, *22*, 55–81.
(9) Dabrowski, J. *Methods Enzymol.* **1989**, *179*, 122–156.
(10) Scarsdale, J. N. NMR Studies of Ganglioside Conformation; Ph.D. Dissertation, Yale University, 1989.

0002-7863/91/1513-1987$02.50/0

solubilization approach can, however, be challenged because it is possible that the three-dimensional structure of the sugar portions of biological glycoforms is influenced by local interaction of the oligosaccharide with its membrane or protein environment.[12,13]

One approach that is applicable in a membrane environment is that of solid-state or liquid-crystal NMR. This differs from normal solution NMR in that many of the interactions normally averaged to zero in solution remain finite and are easily observed. ^{2}H NMR is among the most frequently applied techniques in these situations.[14-19] For molecules executing pure axial rotation about a membrane bilayer normal the observed ^{2}H quadrupolar coupling constant may be defined as

$$\Delta\nu = \frac{3}{2}\frac{e^2qQ}{h}S_{\text{bilayer}}S_{\text{mol}}\left(\frac{3\cos^2\theta - 1}{2}\right) \quad (1)$$

where e^2qQ/h is the quadrupolar coupling constant (assumed to be 170 kHz for sp^3 C–D bonds in this study) and θ is the angle between the C–D bond axis and a molecule fixed director. S_{bilayer} is an order parameter that describes the degree of order and orientation of the bilayer director (i.e., the normal). S_{bilayer} approaches 0 if a bilayer fragment tumbles isotropically and a finite value if a higher degree of order is present. For bilayers with perfect unidirectional order in which the bilayer normal is parallel to the magnetic field S_{bilayer} becomes 1, while for perfectly ordered bilayers in which the normal is perpendicular to the field S_{bilayer} becomes −0.5. S_{mol} describes the motional deviation of the molecule fixed director from a perfectly ordered position with respect to the bilayer director axis. Both S_{mol} and S_{bilayer} will be identical for multiple deuterons or dipolar coupled spins on an internally rigid structure associated with the bilayer. Equation 1 is expected to be strictly valid only for bilayers and molecules with a high degree of cylindrical symmetry. However, lack of data has required assumptions of this form in all but a few cases.

To date, the application of anisotropic NMR to the carbohydrate moieties of membrane-bound glycoforms has been limited almost solely to ^{2}H NMR studies of simple ceramide or dialkylglycero mono- or disaccharides. One set of studies has focused on, or made use of, relaxation measurements which can supplement information extractable from quadrupolar splittings.[20-22] Other studies have relied almost entirely upon utilization of expressions analogous to eq 1 and thus depend on the validity of the related assumptions.[23-28] In these studies, the directions of all C–D bonds are assumed fixed in the molecular frame and only the carbohydrate ring orientation and one order parameter need to be determined. Orientational space is typically sampled by reorientation of the molecular director in the molecular frame of reference to find orientations which, in combination with eq 1, reproduce the set of quadrupolar splittings. The structures produced in these studies are very reasonable, but often require intuitive or computational judgments to choose among formally valid solutions. Removing this requirement and relaxing the necessary assumptions about the motional symmetry clearly require additional data.

One way in which additional NMR data constraints could be obtained would be to measure dipolar coupling constants between pairs of nuclei on glycosyl rings. These have a geometry dependence very similar to quadrupolar splitting. For any pair of spin $^1/_2$ nuclei the dipolar coupling interaction results in a coupling of

$$D_{ij} = \frac{\gamma_i\gamma_j h}{\pi^2 r^3}S_{\text{bilayer}}S_{\text{mol}}\left(\frac{-3\cos^2\theta + 1}{2}\right) \quad (2)$$

where γ_i and γ_j are the magnetogyric ratios of the interacting nuclei, i and j, r is their internuclear distance, and the other constants maintain the definitions given for eq 1. The observed coupling constant is actually the sum of the dipolar splitting defined by eq 2 and the through-bond scalar coupling constant.

Although some reports can be found on membrane-related work,[25] ^{2}H–^{2}H and ^{2}H–^{1}H dipolar splittings usually do not exceed ^{2}H NMR line widths and are thus difficult to measure. ^{1}H–^{1}H interactions are often large and are exceedingly difficult to measure except in special cases.[29] This arises because of strong coupling between multiple protons, near degeneracy of the chemical shifts for the protons on the glycosyl rings, and a dominant background from the lipid matrix in which the molecule of interest is solubilized. ^{13}C–^{13}C and ^{13}C–^{1}H dipolar interactions are perhaps the most accessible. If all sites in a glucose ring were labeled and all interactions were observable, nearly 50 noncollinear vectors would be available for determination of orientation and order parameters. Such additional information would allow the assumption of axially symmetric motion to be relaxed.

For the more general case where the motional averaging around the director axis is not axially symmetric and the molecule tends to wobble in a preferred direction with respect to its own molecular axes, the $S_{\text{mol}}(-3\cos^2\theta + 1)/2$ term of eqs 1 and 2 must be replaced with[30]

$$A_{zz}S_{zz} + \tfrac{1}{3}(A_{xx} - A_{yy})(S_{xx} - S_{yy}) + \tfrac{4}{3}A_{xy}S_{xy} + \tfrac{4}{3}A_{xz}S_{xz} + \tfrac{4}{3}A_{yz}S_{yz} \quad (3)$$

where

$$A_{p,q} = (3\cos\alpha_p\cos\alpha_q - \delta)/2 \quad (4)$$

and

$$S_{p,q} = \langle(3\cos\theta_p\cos\theta_q - \delta)/2\rangle \quad (5)$$

The $\cos\alpha_p$ are the direction cosines defining the orientation of the internuclear vector relative to a molecule fixed frame, and the $S_{p,q}$ are molecular order parameters describing the average order of the molecular axes, p,q, with respect to the director (i.e., the bilayer normal) in terms of direction cosines. The $S_{p,q}$ are the elements of what is known as an order matrix,[31] which has nine total elements, five of which are independent. This matrix can be diagonalized by locating the principal axes of the order tensor in the molecular frame. The new elements, $S_{x',x'}S_{y',y'}$ and $S_{z',z'}$, give the degree of molecular order around each of the three axes of the new principal frame of reference.

(11) Yu, R. K.; Koerner, T. A. W.; Scarsdale, J. N.; Prestegard, J. H. *Chem. Phys. Lipids* **1986**, *42*, 27–48.
(12) Carver, J. P.; Michnick, S. W.; Imberty, A.; Cumming, D. A. *Carbohydrate Recognition and Cellular Function*; CIBA Foundation Symposium 145; Bock, G., Harnett, S., Eds.; Wiley: New York, 1989; pp 6–26.
(13) Cumming, D. A.; Shah, R. N.; Krepinsky, J. P.; Grey, A. A.; Carver, J. P. *Biochemistry* **1987**, *26*, 6655–6663.
(14) Seelig, J.; MacDonald, P. M. *Acc. Chem. Res.* **1987**, *20*, 221–228.
(15) Seelig, J. *Q. Rev. Biophys.* **1977**, *10*, 353–418.
(16) Smith, I. C. P. *Biomembranes* **1984**, *12*, 133–168.
(17) Davis, J. H. *Biochim. Biophys. Acta* **1983**, *737*, 117–171.
(18) Griffin, R. G. *Methods Enzymol.* **1981**, *72*, 108–174.
(19) Jacobs, R. E.; Oldfield, E. *Prog. NMR Spectrosc.* **1981**, *14*, 113–136.
(20) Renou, J. P.; Giziewicz, J. B.; Smith, I. C. P.; Jarrell, H. C. *Biochemistry* **1989**, *28*, 1804–1814.
(21) (a) Auger, M.; Carrier, D.; Smith, I. C. P.; Jarrell, H. C. *J. Am. Chem. Soc.* **1990**, *112*, 1373–1381. (b) Auger, M.; Van Calsteren, M.-R.; Smith, I. C. P.; Jarrell, H. C. *Biochemistry* **1990**, *29*, 5815–5821.
(22) Speyer, J. B.; Weber, R. T.; Das Gupta, S. K.; Griffin, R. G. *Biochemistry* **1989**, *28*, 9569–9574.
(23) Skarjune, R.; Oldfield, E. *Biochemistry* **1982**, *21*, 3154–3160.
(24) Jarrell, H. C.; Giziewicz, J. B.; Smith, I. C. P. *Biochemistry* **1986**, *25*, 3950–3957.
(25) Jarrell, H. C.; Jovall, P. A.; Giziewicz, J. B.; Turner, L. A.; Smith, I. C. P. *Biochemistry* **1987**, *26*, 1805–1811.
(26) Jarrell, H. C.; Wand, A. J.; Giziewicz, J. B.; Smith, I. C. P. *Biochim. Biophys. Acta* **1989**, *897*, 69–82.
(27) Auger, M.; Smith, I. C. P.; Jarrell, H. C. *Biochim. Biophys. Acta* **1989**, *981*, 351–357.
(28) Carrier, D.; Giziewicz, J. B.; Moir, D.; Smith, I. C. P.; Jarrell, H. C. *Biochim. Biophys. Acta* **1989**, *983*, 100–108.
(29) Higgs, T. P.; MacKay, A. L. *Chem. Phys. Lipids* **1977**, *20*, 105–114.
(30) Strenk, L. M.; Westerman, P. W.; Doane, J. W. *Biophys. J.* **1985**, *48*, 765–773.
(31) (a) Saupe, A. *Z. Naturforsch.* **1964**, *19A*, 161–171. (b) Engel, A. K.; Cowburn, D. *J. Biomol. Struct. Dyn.* **1983**, *1*, 319–335.

In this paper we examine the structure of a simple glycolipid analogue β-dodecyl glucoside (BDOG) whose molecular shape is clearly noncylindrical, suggesting that eqs 1 and 2 are not applicable. While BDOG is not actually a natural glycolipid, it represents one of a number of alkyl glycosides finding broad application as a nondenaturing detergent in biochemistry. We demonstrate that by choice of a suitable model membrane system (one that is oriented), uniform ^{13}C labeling of the glucose ring and application of both 1- and 2-dimensional NMR pulse methods, enough ^{13}C–^{13}C and ^{13}C–^{1}H dipolar splittings can be measured to allow determination of the order matrix elements. Additional measurement of a few deuterium quadrupole splittings helped relate these splittings to previous work and to the order of the hydrophobic part of the bilayer. The analysis leads to a fairly explicit description of the average orientation and dynamics of the head group of BDOG. The methodology described should be applicable in a straightforward manner to complex and more biologically relevant glycoforms and may, in many cases, be extended to the study of other membrane-associated species.

The model membrane system utilized is the CHAPSO/DMPC system described in detail elsewhere.[32] This system appears to be composed of discoidal particles that largely maintain the structural properties of pure lipid bilayers in a liquid-crystalline (L_α)-like state. Advantages of utilizing this system lie in two basic properties. First, in the presence of a strong magnetic field the bilayers orient so that the bilayer normals are orthogonal to the field (maximum $S_{bilayer}$ is −0.5). In this sense, the system shares properties with numerous liquid crystals used in spectroscopy that bear less resemblance to biochemical systems.[33-36] Orientation does away with the resolution and sensitivity problems associated with powder patterns, thereby allowing uniform labeling schemes to be optimized and 2-D experiments to be run more quickly. This advantage is similar to that provided by the frequently used glass-plate method of orienting lipid lamellae,[37] but the CHAPSO system provides somewhat higher resolution and sensitivity. A second useful property arises from the fact that $S_{bilayer}$ can be varied somewhat independently of the other terms of eqs 1–5 over a range of about −0.35 to 0.0 by variation of the CHAPSO/DMPC ratio. This allows the experimentalist to work with a sample in which the range of dipolar splittings observed are large enough to be accurately measured but small enough to avoid strong coupling between too large a number of spins. Also, variation of $S_{bilayer}$ allows determination of the signs of some dipolar coupling constants relative to scalar coupling constants. This is of significant value in reducing ambiguities in correlating measured splittings with direction cosines.

Materials and Methods

Materials. DMPC, CHAPSO, *N*-(2-hydroxyethyl)piperazine-*N*′-2-ethanesulfonic acid (HEPES), unlabeled BDOG, and ^{2}H-depleted water were purchased from Sigma (St. Louis, MO). [$^{13}C_6$]Glucose (66% random enrichment at all positions), D_2O, and D_2SO_4 were obtained from MSD Isotopes (Los Angeles, CA); all other reagents used in the syntheses of BDOG were acquired from Aldrich (Milwaukee, WI).

Synthesis of β-D-Dodecyl [$^{13}C_6$]Glucopyranoside. 2,3,4,6-Tetraacetyl-[$^{13}C_6$]glucopyranosyl bromide (65 mg, 0.16 mmol) was synthesized and reacted with 36 μL of dodecanol (0.16 mmol) according to the method of Rosevear et al.[38] The reaction was run at room temperature in 2 mL of 1,2-dichloroethane in the presence of 35 mg of $AgCO_3$, 5 mg of I_2, and 50 mg of 4-Å molecular sieves. After 18 h at room temperature under argon, 12 mL of $CHCl_3$ was added to the reaction mixture which was then filtered and extracted with H_2O. The organic layer was dried with $MgSO_4$, filtered, rotovapped, and flash chromatographed on a 2 × 33 cm silica gel column eluted with 3:1 hexane/ethyl acetate. Silica gel thin-layer chromatography (TLC) using the same solvent system was used to identify fractions containing the β (R_f = 0.41) anomer. Fractions were pooled and rotovapped to isolate the tetraacetate form of BDOG in a 38% reaction yield. Tetraacetyl[$^{13}C_6$]BDOG (30 mg, 60 μmol) was dissolved in 2 mL of methanol and deacetylated by adding 0.2 mL of 1 M sodium methoxide and stirring at room temperature for 0.5 h. The deacetylated mixture was neutralized with 0.2 g of cleaned and dried Dowex 50W-X4-H^+ and flash chromatographed on a 1 × 20 cm column with 4:1 $CH_3OH/CHCl_3$. The pure product was pooled, rotovapped, redissolved in 2:1 dioxane/H_2O, and lyophilized to yield 15 mg of a white powder [$^{13}C_6$]BDOG (98% yield from the tetraacetate). The identity of the product as well as its purity (>95%) was confirmed by both ^{13}C and ^{1}H NMR (in d_6-DMSO).

Synthesis of *1*-d_2- and *2*-d_2-BDOG. *2*-d_2-Lauric acid was prepared by heating lauric acid in D_2SO_4 according to the method of van Heynigen et al.[39] *2*-d_2-Lauric acid (0.5 g) was dissolved in 20 mL of ether containing 0.21 g of lithium aluminum hydride and stirred in an ice bath under dry argon. After warming to room temperature, the mixture was allowed to stir overnight before water was carefully added until the evolution of gas ceased. A thick aqueous precipitate formed. The ether was poured from this mixture, and the solid was then rinsed with ether. The ether layer was rotovapped, and the residue was flash chromatographed on a column eluted with 3:1 hexane/ethyl acetate. *2*-d_2-Dodecanol was thus isolated in near quantitative yield.

1-d_2-Dodecanol was synthesized from unlabeled lauric acid in the same manner except that the reduction was performed by using deuterated lithium aluminum hydride. *1*-d_2- and *2*-d_2-β-dodecyl (2,3,4,6-tetraacetyl)glucopyranoside were then synthesized from the labeled dodecanols by using (trimethylsilyl)trifluoromethanesulfonate according to the method of Ogawa et al.[40] They were purified by flash chromatography, deblocked, and repurified as described for [$^{13}C_6$]BDOG. The overall yields were low (<10%), perhaps because the glycosylation reaction was not run under scrupulously dry conditions.

Semiselective Deuteration of BDOG on the Glucose Ring. Unlabeled BDOG (190 mg) was dissolved in 24 mL of a refluxing 2:1 dimethoxyethane/D_2O mixture containing 3 mL of a D_2O-exchanged slurry of Raney nickel with vigorous stirring according to the method of Renou et al.[20] Six-milliliter aliquots of this mixture were removed at 15 and 45 min and cooled to room temperature while the remainder of the reaction mixture was allowed to react for 2 h (total). The pools were filtered through glass wool, rotovapped, and flash chromatographed on a 1 × 15 cm silica gel column eluted with 4:1 $CHCl_3/CH_3OH$. The major product (R_f = 0.625 on TLC using the above solvent system) was separated from two minor impurities (R_f = 0.70 and 0.55). The amounts of BDOG isolated from the 15-, 45-, and 120-min pools were 36, 28, and 41 mg, respectively.

To establish the levels of deuteration on the glucose rings, about 3 mg each of the deuterated BDOG was acetylated by dissolving in 2 mL of pyridine, adding 0.5 mL of acetic anhydride, and stirring for 8 h at room temperature. After drying in vacuo, the tetraacetyl-BDOG was dissolved in $CDCl_3$ and ^{1}H NMR spectra were acquired. Chemical shift assignment (by selective homonuclear decoupling) was facilitated by the increased dispersion of the chemical shifts of the ring protons of the tetraacetate relative to free BDOG [chemical shifts of the acetate (ppm) glc-1,2,3,4,5,6,6′, 4.47, 4.96, 5.18, 5.06, 3.65, 4.18 (strongly coupled); dodecyl-1,1′, 3.86, 3.45]. On the basis of these assignments and spectral integrations the following percentage deuteration for BDOG was found: 15 min glc2 <5%, glc3 70%, glc4 30%, glc6,6′ <5%; 45 min glc2 10%, glc3 90%, glc4 80%, glc6,6′ 15% × 2; 2 h glc2 25%, glc3 >90%, glc4 90%, glc6,6′ 50% × 2.

Preparation of the CHAPSO/DMPC NMR Samples. CHAPSO and DMPC were weighed into 5-mm NMR tubes along with BDOG and 0.1 M KCl in D_2O for ^{13}C NMR samples. ^{2}H NMR samples were prepared in ^{2}H-depleted H_2O buffered with 0.1 M Na^+HEPES, pH 7.8. Tubes were sealed with Teflon tape, capped, and mixed thoroughly by using a combination of centrifuging, heating, cooling, and vortexing. The structure and dynamics of the bilayers and their associated molecules have been demonstrated[32] to be fairly independent of the percentage (w/v) of total amphiphile (i.e., CHAPSO + DMPC + BDOG) from at least 15% to 50%. We chose to work at 30%. Most experiments were collected at a CHAPSO/DMPC ratio of 1:3 ($S_{bilayer}$ of about −0.25), which provides a good compromise between resolution of chemical shift and magnitude of dipolar coupling.

NMR Methods. All spectra were acquired by using a Bruker AM500 spectrometer (11.7-T magnet) using Bruker DISR88 (Billerica, MA)

(32) Sanders, C. R.; Prestegard, J. H. *Biophys. J.* **1990**, *58*, 447–460.
(33) Emsley, J. W.; Lindon, J. C. *NMR Spectroscopy Using Liquid Crystalline Solvents*; Pergamon Press: Oxford, U.K., 1975.
(34) Emsley, J. W., Ed. *NMR of Liquid Crystals*; Reidel: Dordrect, The Netherlands, 1985.
(35) Forrest, B. J.; Reeves, L. W. *Chem. Rev.* **1981**, *81*, 1–14.
(36) Khetrapal, C. L.; Kunwar, A. C. *Adv. Magn. Reson.* **1977**, *9*, 301–422.
(37) Moll, F.; Cross, T. A. *Biophys. J.* **1990**, *57*, 351–362.
(38) Rosevear, P.; Van Aken, T.; Baxter, J.; Ferguson-Miller, S. *Biochemistry* **1980**, *19*, 4108–4115.
(39) Van Heynigen, W. E.; Rittenberg, D.; Schoenheimer, R. *J. Biol. Chem.* **1938**, *125*, 495–500.
(40) Ogawa, T.; Beppu, K.; Nakabayashi, S. *Carbohydr. Res.* **1981**, *93*, C6–C9.

software. Most spectra were acquired at 40 °C. Liquid-crystalline samples were not spun and were examined in the absence of a field frequency lock. The drift of the magnet under such conditions was observed to be <1 Hz in 8 h and was thus too small to be of significance in our studies.

^{2}H NMR spectra were obtained by using a 5-mm high-resolution ^{1}H probe pulsing through the lock channel (90° ^{2}H pulse, 20 μs) and a solids echo pulse sequence described by Miner et al.[41] Pulse repetition times were always >70 ms. ^{13}C spectra were acquired by using a 5-mm high-resolution ^{13}C/^{1}H dual probe (90° ^{13}C pulse, 6.2 μs). ^{1}H decoupling was executed by using the WALTZ sequence[42] with 40-W power (^{1}H 90° decoupler pulse, 23 μs). When decoupling was utilized, the pulse cycle repetition time was always set to 1.5 s or more (for a duty cycle of <10%) to avoid overheating. The T_1 values of the various glucose carbons in the liquid-crystal samples were estimated to be <0.5 s by finding the null signal in an inversion recovery experiment.[43] When ^{1}H decoupling was not used, the pulse repetition time was always >0.7 s.

Two-dimensional double quantum NMR spectra were obtained by using the sequence[44]

$$90_x\text{-}\tau\text{-}180_y\text{-}\tau\text{-}90_x\text{-}t_1\text{-}90\text{-FID} \quad (6)$$

Two-dimensional double quantum filtered COSY was run by using the time proportional phase incremented version of this experiment.[45,46] To eliminate ^{1}H homonuclear coupling while observing ^{13}C–^{1}H coupling in 1-D ^{13}C spectra or 2-D COSY,[47,48] spectra were acquired with application of the semiwindowless MREV-8 cycle:[48-50]

$$-(90_x\text{-}90_y\text{-}\tau\text{-}90_{-y}\text{-}90_{-x}\text{-}\tau\text{-}90_{-x}\text{-}90_y\text{-}\tau\text{-}90_{-y}\text{-}90_x\text{-})_n- \quad (7)$$

Here, τ is equal to the 90° ^{1}H pulse length (i.e., 23 μs), and $n \times 12 \times \tau$ is equal to the acquisition time. Two-dimensional NMR data were transferred to a VaxStation 3200 computer and processed by using FTNMR software (Hare Research, Woodinsville, WA).

Determination of the Order Matrix Elements and Graphical Generation of Resulting Structures. The program ORDERTEN was written in FORTRAN to search for order tensor elements consistent with the full set of quadrupolar and dipolar couplings determined from NMR experiments. This program calculates a set of direction cosines (see eq 5) for the internuclear vectors taken from a glycolipid structure minimized with the program AMBER.[51-53] The program then increments the five independent order matrix elements, saving combinations that reproduce the experimental data within a user-specified root-meaned-squared (rms) deviation. The order parameters in the principal axis system $S_{x'x'}$, $S_{y'y'}$, and $S_{z'z'}$ and the coordinates of the principal axis frame in the molecular frame are produced by diagonalizing each acceptable order matrix using the Jacobi method.

The structures shown in this paper were produced with the help of a molecular graphics program URANUS (Simon Kearsley) which allowed rotation about the C1–O and O–C1′ bonds (ϕ and ψ) to align the extended dodecyl chain with the principal order axis as defined in the frame of the glucose ring.

Solution of the Structure by the "NMR–Pseudoenergy Approach". For comparison to previous protocols that rely on assumed axial symmetry, we also incorporated the NMR dipolar and quadrupolar data constraints into an NMR–pseudoenergy function in the force field of AMBER and searched for a suitable structure by minimization of the total energy. The protocol and the pseudoenergy terms have been described in detail elsewhere.[53-55]

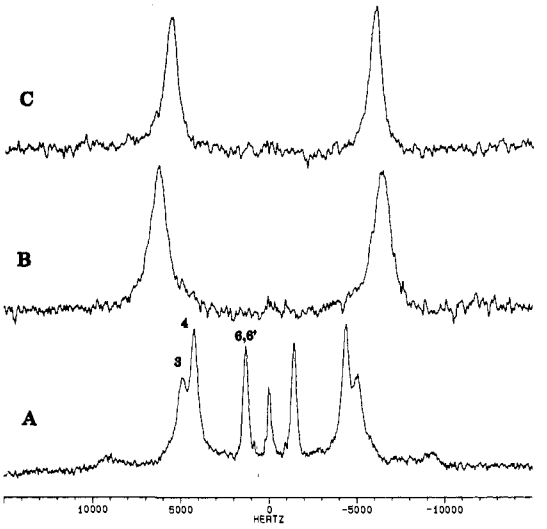

Figure 1. ^{2}H NMR (77 MHz) spectra of deuterated BDOG in 1:3 CHAPSO/DMPC (mol/mol), 30% total lipid (w/v, DMPC + CHAPSO + BDOG), in 100 mM Na^+HEPES, pH 7.8, at 40 °C. (A) BDOG deuterated by 2 h of reaction in the presence of Raney nickel. The sample volume was 0.45 mL and contained 4–5 mg of BDOG. The spectrum was produced following exponential multiplication of the free induction decay (FID) with 40-Hz line broadening. (B, C) d_2-BDOG labeled at the 1- and 2-positions of the alkyl chain, respectively. Samples contained 4 mg of BDOG in 0.41-mL volumes. Spectra were produced with 75-Hz line broadening.

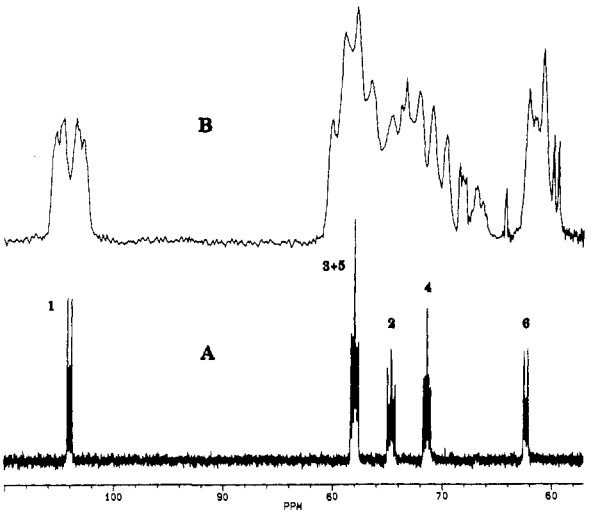

Figure 2. ^{1}H-Decoupled ^{13}C NMR (125.77 MHz) spectra of $^{13}C_6$-BDOG. (A) BDOG in d_6-dimethyl sulfoxide at room temperature. (B) Glucose ring region and BDOG in 1:3 CHAPSO/DMPC, 30% total lipid, 0.1 M KCl, in D_2O at 40 °C. The sample contained 12 mg of BDOG in a 0.55-mL total sample volume. The spectra were produced with 1- and 5-Hz line broadening [for (A) and (B), respectively]. In these spectra and the others presented in this paper, the glcC1 resonance is used as the chemical shift reference and is set to 104 ppm (Bock and Thogersen, 1982).

Results and Discussion

Measurement of ^{2}H Quadrupolar Splittings. The ^{2}H NMR spectrum of BDOG deuterated on the glucose ring and associated with the oriented DMPC/CHAPSO bilayers is shown in Figure 1A. The assignments of the 3,4 and 6 deuterons were unam-

(41) Miner, V. W.; Tyrell, P. M.; Prestegard, J. H. *J. Magn. Reson.* **1983**, *55*, 438–452.
(42) Shaka, A. J.; Keeler, J.; Freeman, R. *J. Magn. Reson.* **1983**, *53*, 313–340.
(43) Sanders, J. K.; Hunter, B. K. *Modern NMR Spectroscopy*; Oxford University Press: Oxford, U.K., 1987.
(44) Mareci, T. H.; Freeman, R. *J. Magn. Reson.* **1983**, *51*, 531–535.
(45) Marion, D.; Wuthrich, K. *Biochem. Biophys. Res. Commun.* **1983**, *113*, 967–974.
(46) Rance, M.; Sorensen, O. W.; Bodenhausen, G.; Wagner, G.; Ernst, R. R.; Wuthrich, K. *Biochem. Biophys. Res. Commun.* **1983**, *117*, 479–485.
(47) Nagayama, K.; Kumar, A.; Wuthrich, K.; Ernst, R. R. *J. Magn. Reson.* **1980**, *40*, 321–334.
(48) Rhim, W.-K.; Elleman, D. D.; Vaughn, R. W. *J. Chem. Phys.* **1973**, *58*, 1772–1773.
(49) Mansfield, P.; Orchard, M. J.; Stalker, D. C.; Richards, K. H. B. *Phys. Rev.* **1973**, *7*, 90–105.
(50) Webb, G.; Zilm, K. W. *J. Am. Chem. Soc.* **1989**, *111*, 2455–2463.
(51) Weiner, P. K.; Kollman, P. A. *J. Comput. Chem.* **1981**, *2*, 287–303.
(52) Weiner, P. K.; Singh, U. C.; Kollman, P. A.; Caldwell, J.; Case, D. A. AMBER, version 3.0, University of California, San Francisco, 1986.
(53) Ram, P. Conformational Studies of Membrane Bound Molecules Using NMR-Molecular Modelling Methods; Ph.D. Dissertation, Yale University, 1989.
(54) Ram, P.; Prestegard, J. H. *J. Am. Chem. Soc.* **1988**, *110*, 2383–2388.
(55) Ram, P.; Mazzola, L.; Prestegard, J. H. *J. Am. Chem. Soc.* **1989**, *111*, 3176–3182.

Table I. Experimental and Calculated Dipolar/Quadrupolar Coupling Constants for BDOG in 30% 1:3 CHAPSO/DMPC at 40 °C

nuclear vector	obsd coupling constant	corrected coupling constant	order matrix predicted coupling constants[a]			AMBER minimized
			A	*B*	*C*	
C3–D	9950	9950 ± 1000	9369	9049	8901	(scaling vector)
C4–D	8650	8650 ± 500	8152	8443	8335	7788
C1′–D,D	12600	|12600 ± 1000|				12136/12600
C2′–D,D′	11500	|11500 ± 700|				12165/12282
C6–D,D′	2700	|2700 ± 500|				
C1–C2	262	220 ± 10	232	224	248	219
C3–C4	185	−225 ± 20	−228	−223	−244	−206
C4–C5	305	265 ± 25	281	250	276	269
C5–C6	175	−219 ± 10	−236	−214	−236	−211
C1–C3	100	|100 ± 15|	81	73	83	102
C1–C4	42	|42 ± 15|	33	28	29	44
C4–C6	0	0 ± 15	9	6	7	19
C1–H1	1250	−1420 ± 250	−1237	−1412	−1378	−2042
C2–H2	1375	−1520 ± 250	−1515	−1379	−1635	−2078
C4–H4	1265	−1410 ± 250	−1484	−1536	−1517	−1413
C5–H5	1285	−1430 ± 250	−1579	−1565	−1549	−1851
C6–H6	3150					

[a] *A*, *B*, and *C* refer to the three lowest rms deviation solutions obtained by the order matrix approach (normalized rms deviations 0.0058, 0.0059, and 0.0059, respectively).

biguously made on the basis of integration of the doublets in this spectrum along with doublets in spectra containing BDOG deuterated for 15 and 45 min (not shown) and comparison of these integrals with the levels of deuteration determined by ^{1}H NMR (see Materials and Methods). The level of deuteration of ^{2}H-2 is only 25% in the sample examined in Figure 1A, and its resonance is probably obscured by superposition of the resonances from the nearly completely deuterated 3- and 4-positions. Note that all splittings of ring deuterons are expected to be similar since all C–D bonds are nearly collinear in the favored $^4C_1$(D) ring conformation. The broad doublet of about 18 kHz could be an impurity or may be the 0° edge arising from residual unoriented material. Parts B and C of Figure 1 show the spectra of BDOG in the bilayer system specifically deuterated at the first and second methylenes of the dodecyl chains near the glucose ring. The coupling constants determined from these spectra are listed in Table I. It is interesting to note that the diastereotopic pairs of deuterons at glc6,6′, dodecyl 1,1′, and dodecyl 2,2′ have degenerate splittings. This degeneracy may be an accidental consequence of a particular fixed geometry but more likely results from motional averaging of the splittings of the symmetry-related deuteron pairs. The additional degrees of freedom relative to the glucose ring suggested by the latter interpretation prevent direct use of these data in the order matrix analysis.

Measurement of ^{13}C–^{13}C Dipolar Coupling Constants. The ^{1}H-decoupled spectrum of [$^{13}C_6$]BDOG is shown in Figure 2A. Assignments are made on the basis of those for β-methylglucose.[56] The doublets with ca. 40-Hz splitting arise from one bond scalar coupling between ^{13}C pairs. The singlets in the middle of the doublets in Figure 2A are the consequence of utilizing only partially labeled material.

When placed in the oriented liquid crystal, the spectrum of BDOG changes dramatically. Figure 2B illustrates the glucose region of the ^{13}C spectrum of BDOG in the liquid-crystalline bilayers. While the C1 resonance remains well-resolved from other peaks, it is now broad and complex. Resolution enhancement shows that this resonance is composed of at least three pairs of lines (J_{eff} ca. 250, 100, and 45 Hz). This indicates that C1 experiences a significant dipolar coupling to at least three other carbons. One of these is almost certainly C2, and the effective coupling to that carbon will be the sum of the dipolar and scalar coupling constants. The others must arise from long-range (through-space) dipolar interactions since two-bond carbon–carbon scalar coupling constants are too small to be significant in the oriented media. The line widths of the individual peaks are in the neighborhood of 50 Hz, much broader than in isotropic solution

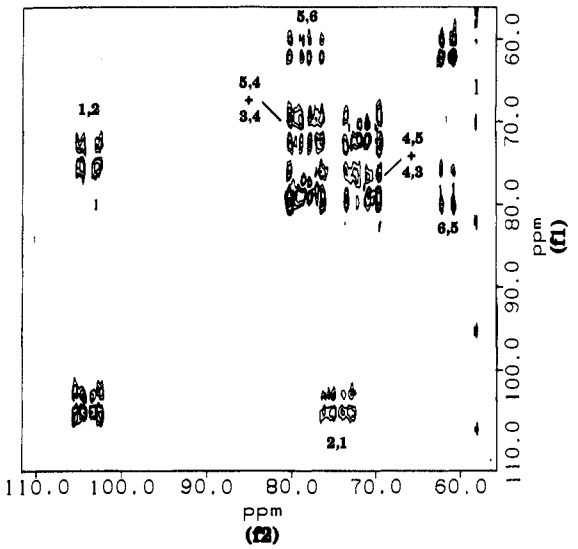

Figure 3. ^{1}H-Decoupled double quantum filtered COSY of $^{13}C_6$-BDOG in 1:3 CHAPSO/DMPC, 30% total lipid, at 40 °C. The sample contained 7 mg of BDOG in a volume of 0.35 mL. 64 t_1 points with spectral sizes of 1024 points were acquired with 380 scans per t_1 value separated by a fixed delay of 2.5 s between scans. The spectral width in both dimensions was 7042 Hz. FIDs were apodized in both f_1 and f_2 prior to Fourier transformation by zero-filling, skewed sine-bell multiplication, and exponential multiplication. Labeled crosspeaks indicate the glucose carbons giving rise to the active coupling, with the first number indicating at which carbon resonance the peak appears in f_2.

due to reduced motion and, probably, unresolved long-range dipolar interactions. The C2–C6 portion of spectrum 2B is very complex and is, to a certain extent, confused by natural abundance resonances from the liquid-crystal matrix.

The ^{1}H-decoupled double quantum filtered ^{13}C COSY spectrum of BDOG in the CHAPSO/DMPC system is shown in Figure 3. Use of a double quantum filter eliminated all natural abundance ^{13}C resonances, and the fairly short t_1 evolution time prevents direct observation of crosspeaks from pairs with smaller couplings. The C2–C6 region is now largely interpretable. C1–C2 crosspeaks are observed with a fairly large active coupling along with multiple passive couplings. Continuation of the correlation from C2 to C3 cannot, however, be accomplished because the C2–C3 crosspeaks cannot be unambiguously identified.

Beginning at the well-resolved C6 peak, C5–C6 crosspeaks are observed with no significant passive coupling at the C6 position (indicating D_{C4-C6} is ca. 0). A large passive coupling is observed at C5 which, by its size, can only be D_{C5-C4}. The C5–C4 crosspeak

(56) Bock, K.; Thogersen, H. *Annu. Rep. NMR Spectrosc.* **1982**, *13*, 1–57.

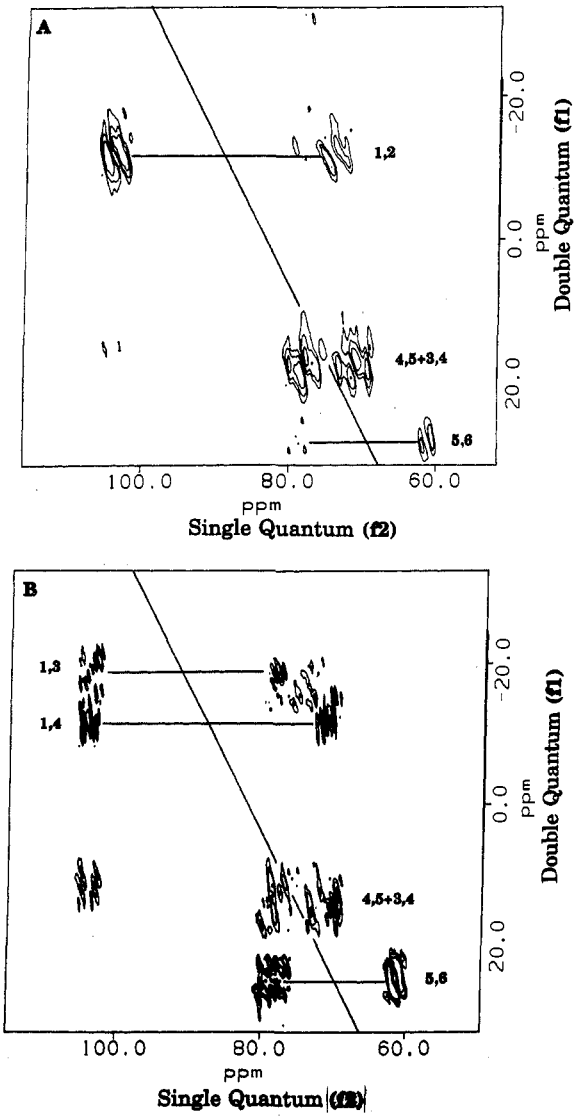

Figure 4. ^{1}H-Decoupled double quantum NMR spectra of $^{13}C_6$-BDOG in the liquid-crystalline bilayers at 40 °C. The sample utilized was that described in the legend of Figure 2B. (A) Experiment optimized for 350-Hz coupling by τ = 710 μs. 30 t_1 points were acquired with t_1 increments of 125 μs and an f_2 sweep width of 8065 Hz. 512 (×2 real/imaginary) scans per t_1 point were averaged with 1.5-s delays between pulse cycles. (B) Experiment run with τ selected for optimal excitation of double quantum coherence, where J_{eff} is 70 Hz. 32 t_1 points were taken with sweep widths in both f_1 and f_2 of 8196 Hz, 127 Hz/point and 8196 Hz. 768 (×2) scans separated by 2-s delays were acquired per t_1 point.

can be identified at the C4 f_2 resonance position and associated with a fairly large C4–C3 passive coupling. The actual C4–C3 crosspeaks are obscured by the C4–C5 peaks and probably by internal cancellation due to its particular set of active and passive interactions. The ca. 100-Hz long-range coupling to C1 inferred by resolution enhancement of (B) in Figure 2 corresponds to a C1–C(3 or 5) crosspeak which is partly obscured by C1–C2 and is just barely observable in Figure 3. Because the C5–C6 crosspeak at the C5 f_2 position in this experiment and in subsequent double quantum experiments is in no case observed to undergo a passive coupling approaching 100 Hz, this splitting can be assigned to C1–C3. Measurement of all of the coupling constants revealed in this COSY experiment were made by examination of resolution-enhanced rows (the digital resolution in f_1 was too low to allow accurate measurement in this dimension).

We sought a confirmation of the assignments and additional measurements of effective coupling constants by running 2-D double quantum NMR experiments. The two-dimensional double quantum pulse sequence (6) employs a delay, τ, which allows for

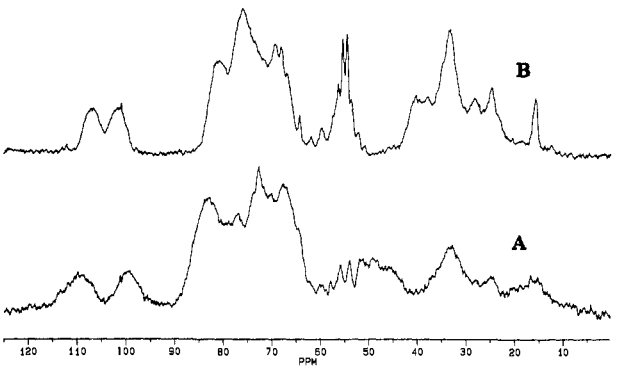

Figure 5. Glucose and aliphatic region of the ^{1}H-coupled spectrum of BDOG and the liquid crystal at 40 °C. (A) Spectrum from a 0.55-mL sample containing 12 mg of BDOG in 1:3 CHAPSO/DMPC, 30% total lipid. (B) Spectrum acquired in the presence of the semiwindowless MREV-8 sequence (7) with sample conditions the same as (A) except that 7 mg of BDOG were present in a 0.41-mL sample. Both spectra were produced following 20-Hz exponential line broadening.

emphasis of coupling constants of various sizes. We ran three experiments using τ chosen to optimally excite resonances involved in coupling constants of 350, 150, and 70 Hz. The results of the two extremes are shown in Figure 4. The projection of data onto the f_2 axis of these two-dimensional spectra is equivalent to a 1-D INADEQUATE spectrum,[57] while the f_1 dimension yields pairs of peaks at the sum of chemical shifts (relative to the f_2 offset frequency) symmetrically disposed about the $\omega_1 = 2\omega_2$ diagonal.[58] The short (J_{opt}=350) τ spectrum is shown in Figure 4A and, along with the intermediate τ run (data not shown), confirms the interpretation of the COSY experiment for C1–C2, C3–C4, C4–C5, C5–C6, and C4–C6. The long τ experiment reduced the amplitude of the C1–C2 crosspeaks and allowed observation of C1–C3 and C1–C4 crosspeaks.

A ^{1}H-decoupled J-resolved experiment was also successfully run (data not shown), which further confirmed the interpretation of the COSY and double quantum experiments. In addition, this spectrum revealed a large (100–200 Hz) coupling to C2 in addition to that of C1–C2, suggesting the C2–C3 interaction is not insignificant. Reexamination of the COSY and double quantum data resulted in identification of patterns consistent with this interpretation. However, the difficulty in quantitating such peaks in those experiments due to antiphase cancellation and spectral overlap suggests caution in interpretation.

The effective ^{13}C–^{13}C coupling constants are reported in Table I. Most of these constants were measured multiple times in multiple experiments so, where possible, errors are given as standard deviations for those measurements. A more conservative approach is to set the error at $\pm^1/_2$ the line widths—approximately 25 Hz.

^{13}C chemical shift anisotropies can be measured by comparing the chemical shifts observed in the above set of experiments with the isotropic values which can be obtained either by heating the sample above 50 °C or by adding CHAPSO (see Figure 7). Because the chemical shift anisotropy tensor has been determined for glucose 1-phosphate,[59] these measurements are potentially a source of additional orientational constraints. At this time we have not incorporated these data into our analysis, but note their possible utility.

Measurement of ^{13}C–^{1}H Dipolar Splittings. Figure 5A shows the ^{1}H-coupled spectrum of [$^{13}C_6$]BDOG (glucose region) in the oriented lipid system. The large splitting observed for C1 is due to dipolar plus scalar coupling to H1. Each peak of the resonance is the entire C1 multiplet of Figure 2A broadened by additional long-range C1–^{1}H coupling. In addition to the poor resolution

(57) Bax, A.; Kempsall, Freeman, R. *J. Magn. Reson.* **1980**, *41*, 349–353.
(58) Braunschweiler, L.; Bodenhausen, G.; Ernst, R. R. *Mol. Phys.* **1983**, *48*, 535–560.
(59) McDowell, C. A.; Naito, A.; Sastry, D. L.; Takegoshi, K. *J. Magn. Reson.* **1988**, *78*, 498–510.

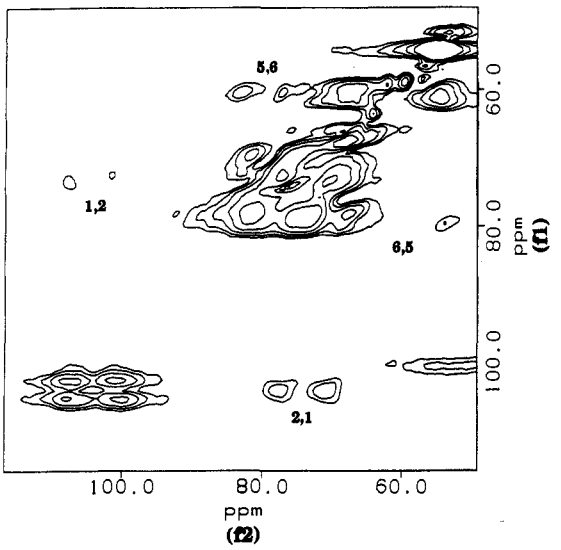

Figure 6. Magnitude COSY ^{13}C spectrum of bilayer-associated $^{13}C_6$-BDOG acquired with ^1H-decoupling in f_1 and semiwindowless MREV-8 ^1H–^1H homodecoupling in f_2. 46 t_1 points were taken with an increment of 118 μs. The f_2 sweep width was 13 900 with a spectral size of 2048. 606 scans per t_1 point were taken with a delay of 1.5 s between scans. Only the glucose region of the spectrum is shown. The f_2 offset and sweep width were set so that the glucose ring resonances were not affected by foldover of the natural abundance background from the lipid matrix. The sample was examined at 40 °C and contained 1:3 CHAPSO/DMPC, 30% total lipid, 7 mg of BDOG, and a volume of 0.41 mL.

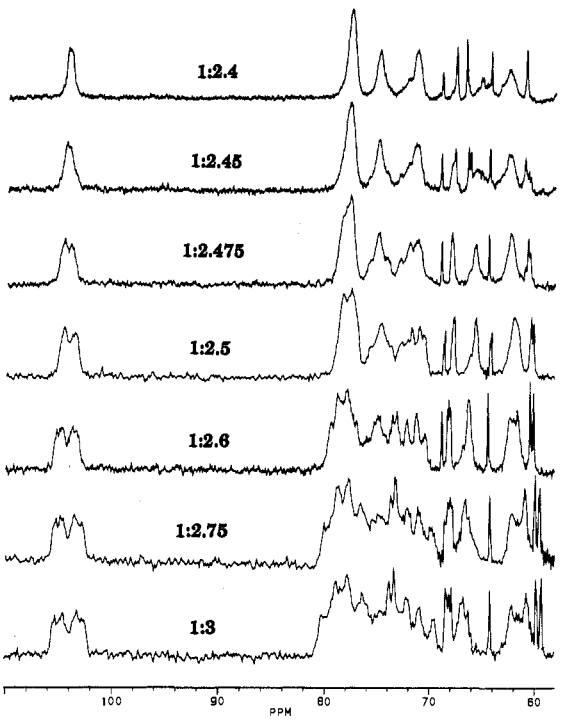

Figure 7. ^1H-Decoupled ^{13}C NMR spectra (glucose region only) during titration of a sample containing 5 mg of $^{13}C_6$-BDOG, 30% total lipid at 40 °C. The spectra are labeled with the CHAPSO/DMPC molar ratio and were produced following zero-filling and exponential multiplication of the FID with 5-Hz line broadening.

observed for C2–C6, measurement of the direct C–H dipolar splittings can be complicated by the probability of strong dipolar coupling among narrowly dispersed protons which will lead to virtual coupling of nondirectly bound protons to the ^{13}C nuclei directly bound to any of the protons in the strongly interacting spin system. In the case of C1–H, the simple primary doublet observed indicates that this is not a problem, probably because H1 is significantly downfield of the H2–H6 envelope. We utilized a two-dimensional experiment to overcome the resolution problem encountered in Figure 5A along with a pulse sequence (MREV-8) designed to selectively remove ^1H–^1H dipolar coupling (Figure 6). ^1H–^1H dipolar homodecoupling can be effected by any one of a number of pulse sequences.[60,61] We utilized the semiwindowless MREV-8 sequence (see Materials and Methods) which, in addition to ^1H–^1H decoupling, theoretically scales down both scalar and dipolar ^{13}C–^1H interactions by a factor of 0.54 and, in practice, by a range of values in the vicinity of this ideal factor.[50,60] We applied this sequence to our sample and obtained the spectrum shown in Figure 5B. The fact that the C1–H1 splitting was reduced by a factor of 0.55 suggests the sequence was working, at least for this particular spin system. We therefore ran a ^{13}C–^{13}C COSY with full ^1H decoupling in f_1 and semiwindowless MREV-8 in f_2. As can be observed in Figure 6, crosspeak doublets are observed in f_2 at the resonant frequencies of C1, C2, C5, and C6, indicating that any virtual coupling to any of these carbons has been effectively removed. The doublet of C1 is observed, in this case, to be scaled down by a factor of 0.59 from its intrinsic value of ca. 1240. Because the magnitudes of the C–H interactions for C2–C5 should be similar to that of C1–H (because of approximate collinearity) and because strong decoupling among protons is observed to be effectively removed, the scaling factor of 0.59 can be applied to C2–H2, C4–H4 (measured on the diagonal), C5–H5, and C6–H6, allowing estimation of the intrinsic $J + D$ C–H coupling constants (Table I). Nevertheless, the uncertainty of this approach may be high. In cases involving spin systems with very different coupling constants and complexity (such as C6–H,H′) the scaling factor for the ^{13}C–^1H interaction will not be the same from system to system if the pulse sequence is not executed in an ideal manner (see Haeberlen[60] for a description of many of the problems encountered). In our case, the rather long 90° ^1H pulses utilized (23 μs) indicates our technique was certainly not ideal, and while it was still effective in this particular case (see above argument), it may prove unsuccessful in more complex systems at this level of technical quality.

Determination of the Absolute Signs of the Coupling Constants. Knowledge of the absolute signs of the dipolar splittings removes a good deal of the ambiguity associated with determination of θ in eqs 1–3 and is also needed to correct the effective coupling constants for directly bound ^{13}C–^{13}C and ^{13}C–^1H by subtraction or addition of the scalar coupling constants to yield the true dipolar coupling values. Neither the ^{13}C nor the ^2H NMR experiments describes thus far allowed determination of absolute or relative signs of the coupling constants measured. Ideally, the double quantum spectrum should yield some of this information, but we were unsuccessful in extracting values from our data. Another possible method for measuring relative signs of COSY-45,[62] which was run but found to be ineffective because the spin system generally fails to have significant passive coupling from the same spin to the two actively coupled spins, giving rise to a particular crosspeak. Given our inability to extract such information using NMR pulse methodology, we turned to manipulation of the sample. One method that has been utilized for this problem in studies of nematic liquid crystals is to gradually scale down the dipolar couplings by making the solution more isotropic.[63] Scalar couplings remain constant during such processes. Therefore, if the splittings pass through a null before reaching the true isotropic value, the scalar and dipolar terms must be of opposite signs.

We can moderate order and approach isotropy by increasing the CHAPSO content to a CHAPSO/DMPC ratio of about 1:2.4. We therefore titrated the 1:3 sample and monitored scaling of

(60) Haeberlen, U. *High Resolution NMR in Solids: Selective Averaging (Advances in Magnetic Resonance, Supplement* 1); Academic Press: New York, 1976.
(61) Mansfield, P. *Philos. Trans. R. Soc. London A* **1981**, *299*, 479–496.
(62) Bax, A. *Two-Dimensional Nuclear Magnetic Resonance in Liquids*; Delft University Press: Dordrect, 1982.
(63) Diehl, P.; Khetrapal, C. L. *NMR: Basic Princ. Prog.* **1969**, *1*, 1–95.

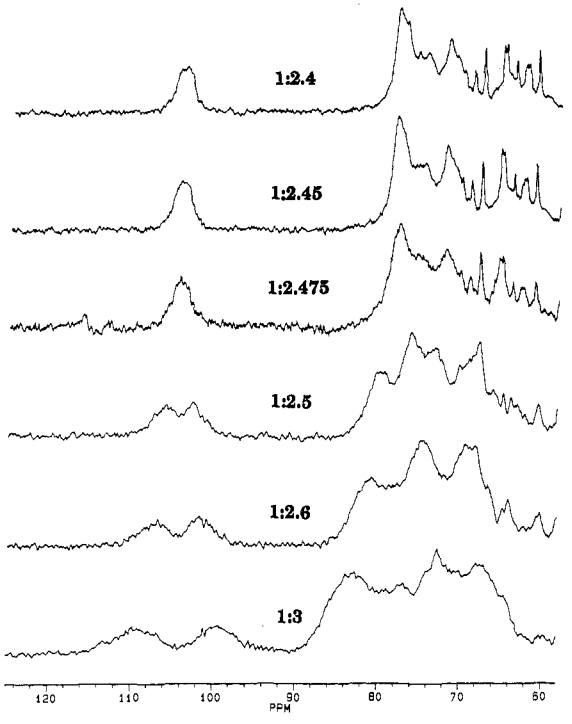

Figure 8. Effect of addition of CHAPSO upon the ^{1}H-coupled ^{13}C spectra of the sample described in the legend of Figure 7. Spectra were produced following 10–20-Hz exponential line broadening.

the splittings with simple ^{1}H-decoupled and coupled ^{13}C NMR as shown in Figures 7 and 8. In the ^{1}H-decoupled series (Figure 7) the C1 resonance (104 ppm) appears to converge smoothly to its final scalar coupling value of +45 Hz[64] without passing through a null. This indicates that the absolute sign of the C1–C2 dipolar coupling constant is also positive. The C6 resonance in Figure 7 (62 ppm) provides a contrasting case. At 1:2.45 resolution enhancement allowed a coupling constant of 45 Hz to be measured: equivalent to J_{C5-C6}. However, at 1:2.475, a sample showing substantial anisotropy as evidenced by the larger coupling of the C1 resonance, resolution enhancement failed to resolve a coupling constant for C6. This indicates that the dipolar coupling constant for C5–C6 is negative. The fact that C1–C2 is nearly collinear with C4–C5 suggests that D_{C4-C5} is also positive, while a similar argument with respect to C5–C6 requires D_{C3-C4} to be negative.

The scalar coupling constant for C1–H1 of β-glucosides is +160.[65] At CHAPSO/DMPC = 1:2.475, resolution enhancement of the C1 doublet of Figure 8 (104 ppm) shows a splitting of no larger than 135 Hz, requiring D_{C1-H} to be negative. Because all of the other C–H bonds of glucose except C6–H,H′ are nearly collinear, they also must possess negative C–H dipolar coupling constants. The full set of corrected data is reported in Table I.

Determination of Average Orientation and Order Matrix for BDOG in the CHAPSO/DMPC Bilayers. Our utilization of NMR data to determine the order matrix for the head group of BDOG is similar to that reported in the literature associated with studies of small organic molecules solubilized in apolar nematic liquid crystals[33,34,36,63] with one general exception. Most such studies focused on molecules possessing internal symmetry axes which allowed for simplification of eq 3 and reduction of the number of independent order matrix elements or utilized two different liquid-crystal matrices having magnetic susceptibilities of opposite sign to effectively double the information available. No such simplifying symmetry elements exist for the head group of BDOG and, at the present time, only the glass plate orientation method would permit control of orientation of the phospholipid lamellae. It is therefore only through the availability of a large number of measured splittings that a general order tensor analysis can be attempted.

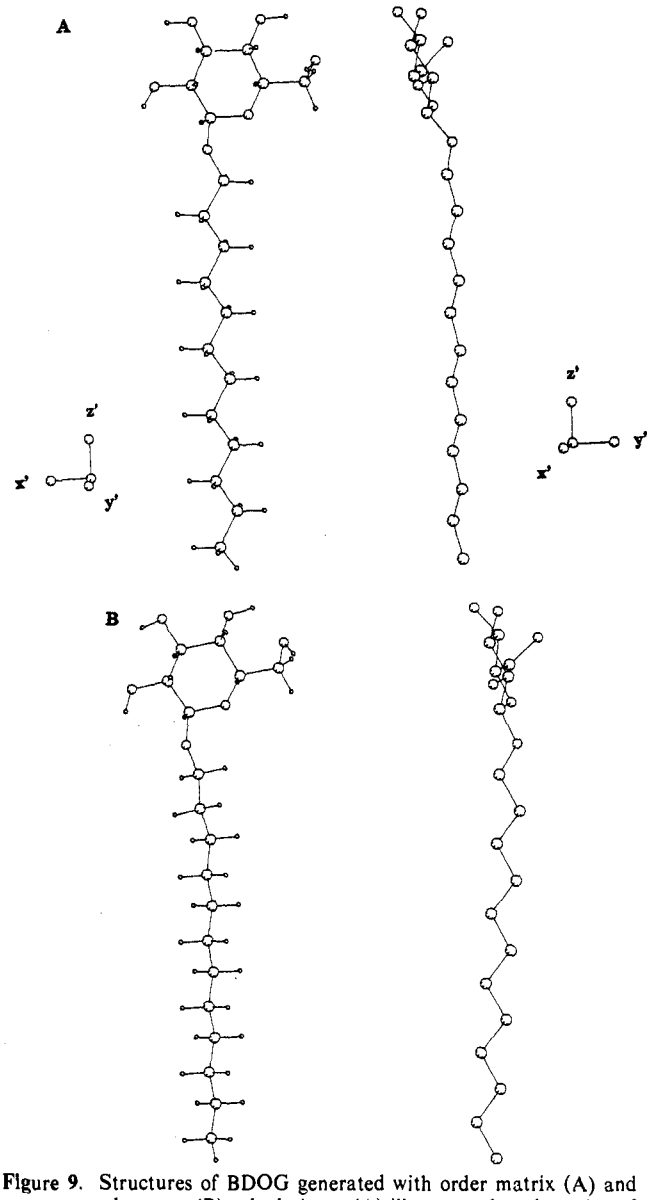

Figure 9. Structures of BDOG generated with order matrix (A) and AMBER pseudoenergy (B) calculations. (A) illustrates the orientation of the glucose ring with respect to the bilayer normal (indicated by z' and the axis of the alkyl chain). The structure represented is that of the lowest rms deviation solution (0.0058). (B) illustrates the minimum energy structure produced by an NMR–pseudoenergy molecular mechanics approach which assumes axially symmetric motions. Hydrogen atoms have been omitted from the view along the approximate plane of the glucose ring for the sake of clarity. Axes for the order tensor are included in (A).

We ran three searches over elements of the order matrix using rough, intermediate, and fine increments of the order matrix elements (0.1, 0.05, 0.03, respectively) and allowed relative rms deviations (0.015, 0.010, and 0.0075). This procedure resulted in 9, 30, and 45 solutions, respectively. Each solution of the order matrix was diagonalized to generate the order parameters $S_{x'x'}$, $S_{y'y'}$, and $S_{z'z'}$ associated with the three principal axes of the order tensor.

The three lowest rms deviations found were 0.0058, 0.0059, and 0.0059. Table I lists the splittings predicted for the corresponding structures. It can be observed that the data are reproduced fairly accurately in each case, with the deuterium data exhibiting the largest disagreement. This may be an artifact of using a slightly different medium in the deuterium NMR samples or a nonexact quadrupolar coupling constant. The axes and head-group orientation for the lowest rms deviation solution are

(64) Krivdin, L. B.; Kalabin, G. A. *Prog. NMR Spectrosc.* **1989**, *21*, 293–488.
(65) Hansen, P. E. *Prog. NMR Spectrosc.* **1981**, *14*, 175–295.

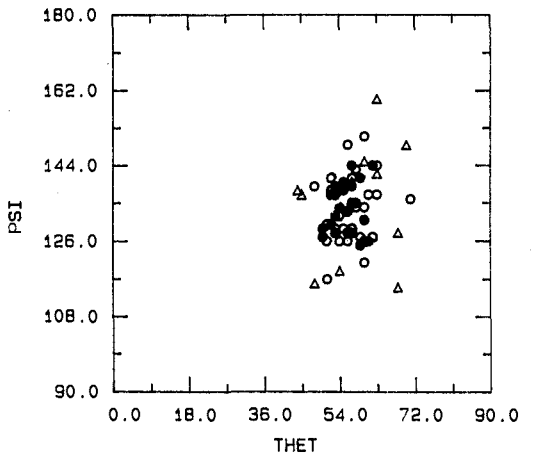

Figure 10. Orientation of the principal order axis in the initial glucopyranosyl coordinate frame. θ is defined as the angle made between the z' principal axis of the order matrix solution and the z axis of the original molecular frame reference z axis, while ψ is the angle between z' and the molecular xy plane. Solutions are shown for relative rms deviations of <0.0075 (solid circles), <0.01 (open circles), and <0.015 (open triangles). Only every other high precision solution is represented.

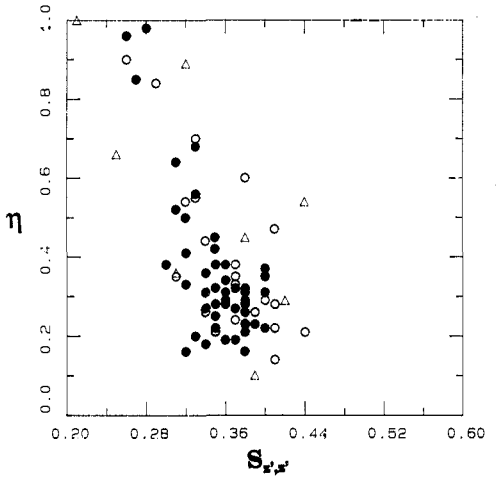

Figure 11. Solutions of the diagonalized order matrix. Order parameters and asymmetry parameters are shown for solutions with relative rms deviations of <0.0075 (solid circles), <0.01 (open circles), and <0.015 (open triangles).

illustrated in Figure 9A. By use of an S_{bilayer} of 0.25, estimated on the basis of direct observation of the DMPC component,[32] the corresponding elements ($S_{z'z'}$, $S_{y'y'}$, $S_{x'x'}$) of the molecular order tensor for the three lowest rms deviation solutions are calculated to be (0.36, −0.22, −0.15), (0.32, −0.23, −0.09), and (0.36, −0.22, −0.15).

In Figures 10 and 11 we attempt to show the precision and degree of correlation in parameters determined. Figure 10 depicts the inclination of the z' principal order axis with respect to the molecular z axis (θ) and the rotation of the z' projection away from the x axis in the molecular xy plane (ϕ). All solutions cluster in a single area with the lower rms deviation solutions near the center (solid circles) and suggest the precision of the axis orientation to be ±15°.

The range of values found for the order tensor elements $S_{x'x'}$ $S_{y'y'}$, and $S_{z'z'}$ associated with the orientations represented in Figure 10 are schematicized in Figure 11 where the asymmetry parameter (η) equals $(S_{x'x'} - S_{y'y'})/S_{z'z'}$. By considering only the solid circles which represent solutions with rms deviations of about 1.5 times the estimated experimental error, it can be observed that solutions for $S_{z'z'}$ are limited to a fairly small range (0.26–0.40), while solutions for η range from 0.15 to nearly 1.0. The wide variation of η is not primarily due to $S_{y'y'}$, which varies only from 0.2 to 0.3, but is mostly the result of a variation of $S_{x'x'}$. This may result from an inadequate number of measurements with high sensitivity to $S_{x'x'}$ or may be a consequence of violation of implicit assumptions such as ring geometry and rigidity. Nevertheless, all solutions indicate a substantial degree of anisotropy of motion ($\eta > 0$).

The orientation is such that the averaged plane of the glucose ring is nearly fully extended from the bilayer but rotated about an axis perpendicular to the effective plane of the ring (approximately the y' axis) such that the 2-hydroxyl does not have to stick into the apolar region of the bilayer. A hydrophobic interaction of the 6-methylene with the membrane may help to bring about the observed orientation. The orientation thus determined is fairly similar to those proposed by Jarrell et al.[24,25] for bilayer-associated β-di(tetradecyl)glycerylglucose and by Skarjune and Oldfield[23] for *N*-palmitoylglucosylceramide except that the glucose rings from the previous studies are rotated so that O5 and OH6 are a little more extended from the bilayer at the expense of a more proximal 2-hydroxyl.

The conformation of the linkage of the glucose ring to the alkyl chain shown in Figure 9A is the only possible conformation allowed using standard bond angles and constraining C1–C12 of the alkyl chain to be coincident with the bilayer normal. The glycosidic angles ϕ and ψ (for dihedral angles defined by H1–C1–O1–C1′ and C1–O1–C1′–C2′) for this structure are 52° and 180°, respectively. The value of ϕ is thus very similar to the normal most favorable value of 60° calculated for simple glucosides.[66] Direct comparison of ψ is difficult since an alkyl chain rather than another sugar is involved in defining this angle. We emphasize that Figure 9A and the structures previously reported represent *averaged* orientations of the ensemble of orientations actually present.

Quantitative interpretation of the order parameters requires an accurate model describing the head-group motions. While the correct model is not known for BDOG, it is qualitatively instructive to consider a simple model in which the head group undergoes excursions from the order axes over a normalized distribution of angles where α_x, α_y, and α_z are the standard angular deviations for each order axis. This treatment has been described in detail elsewhere.[67,68] Using this model and the $S_{z'z'}$, $S_{y'y'}$, and $S_{x'x'}$ for the three best fit solutions, we can determine α_z, α_y, and α_x of about 37°, 43°, and 48–58°, respectively. Although these deviations seem quite large, the order parameters from which they are derived are similar to those determined for other lipids (where it has been assumed that $S_{\text{mol}} = S_{z'z'}$ and $^1/_2 S_{z'z'} = -S_{y'y'} = -S_{x'x'}$). For example, S_{mol} of the most ordered region of the acyl chain region of pure L_α phase phosphatidylcholine bilayers is between 0.4 and 0.5[15,17] and has been observed to range from about 0.2 to 0.45 for β-glucosyl lipids in various L_α lamellar environments.[23-25]

Despite the quantitative differences among the various solution sets of $S_{i'j'}$ the relative magnitudes of $S_{x'x'}$ and $S_{y'y'}$ demonstrate a substantial degree of asymmetric motion for the glucosyl head group. Motion about an axis perpendicular to the average plane of the glucose ring is more restricted than motion about an axis perpendicular to the bilayer normal and approximately parallel to a vector between the C2 and C6 glucose atoms. This would appear to be rather easy to rationalize in a physical–chemical sense. Significant deviation from the displayed orientation by rotation of the glucose ring in its effective plane would cause either the 2- or the 6-hydroxyl to insert into a more apolar region of the bilayer. While this simple model does not take many factors into account, such as steric interactions with the neighboring phospholipids, and while it is not known to what extent the glucose ring itself is inserted into the hydrophobic portion of the bilayers, this model does qualitatively account for the observed order parameters.

Comparison of the Order Matrix with the Single Order Parameter Assumption Approach. As noted in the introduction most prior studies of membrane-associated glycolipids have relied upon

(66) Thogersen, H.; Lemieux, R. U.; Bock, K.; Meyer, B. *Can. J. Chem.* **1982**, *60*, 44–57.
(67) Peterson, N. O.; Chan, S. I. *Biochemistry* **1977**, *16*, 2657–2667.
(68) Bocian, D. A.; Chan, S. I. *Annu. Rev. Phys. Chem.* **1977**, *29*, 307–335.

the assumption that a single order parameter, S_{zz}, adequately describes molecular ordering, allowing the relatively simple eqs 1 and 2 to be applied in structural analysis. Having completed the order matrix approach, we wished to compare these results with those that are obtained if the more restrictive assumptions are employed. We chose to use the NMR-pseudoenergy method incorporating eqs 1 and 2 because it allows for minor adjustment of bond and dihedral parameters from idealized values—a biochemically probable situation. Sixteen starting conformers were used as starting structures, which were generated by four 90° increments of the glycosidic angles ϕ and ψ. The data were input as absolute value splittings with the $^{13}C-^{13}C$ 1 bond, quadrupolar, $^{13}C-^{13}C$ 2 and 3 bond, and $^{13}C-H$ data being weighted by relative factors of 1.85:1.0:0.5:0.004. The size of the weighting factors was such that the pseudoenergy term describing deviation of the experimental data from calculated splittings was generally about half of the total energy of the usual molecular mechanics force field terms. ^2H NMR data for the deuterons of the 1- and 2-positions of the dodecyl chain were included to allow the program to dictate chain geometry. One of the 16 starting structures converged upon a structure whose total real energy and pseudoenergy were, at most, only half of any other final structures and whose total real energy (16 kcal) was only 8 kcal more than that for the structure obtained by minimization in the absence of experimental constraints. Back calculation of the predicted quadrupolar and dipolar splittings yielded splittings of the correct absolute signs, even though this information was not input with the data. However, the agreement of calculated and observed splittings is clearly poorer (Table I) than results from the order matrix approach. This structure is displayed in Figure 9B and possesses an S_{mol} of 0.42 (see eqs 1 and 2). The orientation of the head group with respect to the director is nearly equivalent to that determined by the order matrix approach. Examination of the linkage conformation reveals ϕ and ψ of 37° and 172° with the next two dihedral angles going down the dodecyl group being 170° and -171°. This result suggests that, even for a structure which clearly deviates from simple cylindrical symmetry, utilization of equations such as (1) and (2) can lead to a nearly correct average orientation. While it is difficult to generalize from this one comparison, the calculation does lend support for the use of the simplified equations in cases where adequate orientational data are difficult to obtain.

Conclusions

The experiments described herein demonstrate that with ^{13}C labeling it is possible to generate a considerable body of dipolar coupling data for molecules associated with phospholipid bilayers. The utilization of these data allowed for a more complete description of the structure and dynamics of BDOG than had previously been accomplished for other glycolipids. The results so obtained are more satisfactory not only because of their exactness but because a description of molecular order allows a more explicit physical chemical rationalization of the motional restriction. The methodology employed to facilitate measurement of the dipolar splittings for BDOG should be readily extendable to more complicated membrane-associated glycoforms, although labeling may be restricted by resolution to only one or two of the sugar rings at a time unless more sophisticated NMR techniques are used. Nevertheless, this work certainly represents a logical first step in approaching more complex problems.

Acknowledgment. Financial support of this work was provided by the U.S. Public Health Service (GM19305 and GM33225). Support for C.R.S. was provided by a Public Health Service National Research Award (GM13227-01) from the National Institute of the General Medical Sciences.

NMR and Fluorescence Studies of Cyclodextrin Complexes with Guest Molecules Containing Both Phenyl and Naphthyl Units[1]

Hans-Jörg Schneider,* Thomas Blatter, and Svetlana Simova

Contribution from the FR Organische Chemie der Universität des Saarlandes, D-6600 Saarbrücken 11, FRG. *Received July 12, 1990*

Abstract: The complexation constants of α-, β-, and γ-cyclodextrin (α-, β-, γ-CD's) with 1-anilino-8-naphthalenesulfonate (ANS) and 2-toluidino-6-naphthalenesulfonate (TNS) are (re)evaluated on the basis of different complex and computational models based particularly on NMR titrations. The NMR shifts exerted by the CD's on protons of the guest molecules together with intermolecular NOE's taken from 2D-ROESY spectra give insight into the modes of intracavity inclusion in aqueous solution. In contrast to expectations based on the cavity width α-CD binds phenyl moieties only weakly, whereas β-CD and γ-CD show more or equal intracavity immersion of the smaller phenyl than of the larger naphthalene residues.

Cyclodextrins are increasingly used for enzyme modeling, as catalytic systems, for chromatographic separations, for microencapsulation of drugs, and for many other applications.[2] It is of fundamental importance to develop better methods and a better understanding for the binding modes of substrates within the lipophilic cavities of these cycloamyloses in aqueous solution. Generally one assumes that the inner width of α-cyclodextrin (α-CD, n = 6 glucose units, ~4.5 Å) is suitable for taking up benzene derivatives, whereas β-cyclodextrin (β-CD, n = 7, ~7.0 Å) better accommodates the naphthalenes and γ-cyclodextrin (γ-CD, n = 8, ~8.5 Å) anthracene-type of substrates. The present paper demonstrates that the use of modern NMR techniques in combination with suitable fluorescence and calculational methods can lead to considerable modifications of these seemingly simple rules, if the substrate offers alternatively—or simultaneously—larger and smaller parts for intracavity immersion.

As substrates we have chosen two frequently used fluorescence dyes,[3] namely 1-anilino-8-naphthalenesulfonate (1,8-ANS) and

(1) Host–Guest Chemistry, paper 26. For paper 25, see: Schneider, H.-J.; Blatter, T.; Zimmermann, P. *Angew. Chem., Int. Ed. Engl.* **1990**, *29*, 1161.

(2) (a) Bender, M. L.; Komiyama, M. *Cyclodextrin Chemistry*; Springer: Berlin, 1977. (b) Szeljtli, J. *Cyclodextrin Technology*; Kluwer: Dordrecht; 1988. (c) Saenger, W. *Angew. Chem.* **1980**, *92*, 343; *Angew. Chem., Int. Ed. Engl.* **1980**, *21*, 344. (d) Komiyama, M.; Bender, M. L. In *The Chemistry of Enzyme Action*; Page, M. I., Ed.; Elsevier: Amsterdam, 1984; p 505ff. (e) Bergeron, R. J. In *Inclusion Compounds*; Atwood, J. L., Davies, J. E. D., MacNicol, D. D., Eds.; Academic Press: London, 1984; Vol. III, p 391ff. (f) Yamamoto, Y.; Inoue, Y. *J. Carbohydr. Chem.* **1989**, *8*, 29. These reviews also give detailed accounts on earlier NMR studies of cyclodextrins, although largely restricted to *p*-nitrophenolate complexes. (g) Matsui, Y.; Nishioka, T.; Fujita, T. *Top. Curr. Chem.* **1985**, *128*, 61.

0002-7863/91/1513-1996$02.50/0